Chapter 4

Integration of graphene into a strain-based chemiresistive sensor

While covalent functionalization has become an ubiquitous method to control the physical, optical, and electrical properties of graphene, the inhomogeneity of the distribution of functional groups across the basal plane has stymied the integration of functionalized graphene into commercial devices, which typically require a high degree of fidelity for successful scale-up. Existing methods for covalent functionalization rely on the formation of widespread defects in the pristine graphene basal plane before the attachment of functional groups to the surface, degrading the final quality of the lattice. Thus, researchers have developed new graphene-polymer composites to introduce new functionalities to graphene without destroying the lattice. Polymer composites have the advantage of better reproducibility and strength than either the polymer or graphene alone. These composites have been used successfully in a number of sensor devices, but still rely on integration with oxidized graphene flakes instead of pristine graphene due to the lack of known methods for maintaining the lattice.

Graphene strain sensors are a well-developed area of study but have rarely been used as chemiresistors, in part because the graphene in these sensors is typically integrated with a polymer that does not readily respond to the presence of a vapor (i.e. polydimethylsiloxane (PDMS)). However, strain-based graphene devices, which rely on changes to the resistance of graphene at the surface through increased electron localization, have recently been introduced as a method for the controlled reaction of various molecules with the surface of graphene without permanently damaging the lattice through oxidation. This strain-based approach to altering reactivity is possible, because the graphene lattice can undergo substantial deformation without breaking.[1] When the lattice of graphene is deformed through the application of compressive or tensile strain, the bond lengths with the lattice change based on the direction of the

strain. Tensile strain is of particular interest as it is easier to access experimentally, since current techniques for inducing compressive strain in graphene typically result in permanent wrinkles with no long range order.[2–4] Current transfer methods typically introduce measurable amounts of strain to the lattice. Transmission electron microscopy (TEM) experiments have shown that even pristine graphene suspended away from a substrate contains some number of ripples a few nanometers in height.[2]

In this chapter, a sensor substrate was developed to support graphene as a partially suspended layer above the surface. By suspending the graphene, material is allowed to expand and contract in response to the movement of a polymer overlayer. In this way, the sensor can access both the sensitivity of the graphene and the specific response of different polymers.

Methods

Materials

CVD-grown monolayer graphene on Cu (Cu/Gr) was purchased from Advanced Chemical Supplier Materials (Medford, MA). Grains of graphene from this source are known to be around 50 μm in diameter as reported by the manufacturer. Poly(ethylene-*co*-vinyl acetate) (PEVA, vinyl acetate 18 wt. %) was purchased from Sigma Aldrich. Black Pearls 2000 carbon black (Cabot Co.) were used in the control solutions. All solvents were purchased reagent grade from VWR and used without further purification to generate the vapors tested herein.

Sensor Fabrication

The textured sensor substrates were prepared in a Class 100 cleanroom. Glass slides were first cleaned with acetone and isopropanol before baking at 170°C to remove any residual solvent. Microposit S1813 photoresist (MicroChem) was spun onto the cleaned slide at 500 rpm for 30 s and 4000 rpm for another 60 s followed by a 10 s

exposure to a 425 nm lamp in a contact mask aligner (Suss MicroTech MA6/BA6) through the appropriate mask. The pattern was developed in MF-319 developer (MicroChem) for 90 s. Columns of different heights were grown on the patterned slide by depositing 50 to 300 nm of silicon dioxide with an e-beam evaporator (CHA Industries Mark 40). Lift-off was completed by sonicating the slides at 60°C in Remover PG (MicroChem) for 45 minutes. Contacts were formed by sequentially evaporating 5 nm of Ti, followed by 45 nm of Au, onto masked glass slides. This process produced two metallic electrodes that were separated by a 0.3 cm gap.

Solutions of 4 wt. % PEVA in toluene were sonicated for 2-4 h until the PEVA was well dispersed. To make the coated sensors, a strip of copper covered by monolayer graphene (Cu/Gr) was coated with a supporting layer of PEVA at the selected speed (1000-8000 rpm) for 60 s. The resulting stack (Cu/Gr/PEVA) was then cured for 1 minute at 150°C. Smaller pieces approximately 1 cm x 3 mm (active area ~0.1-0.2 cm^2) were cut and etched in a $FeCl_3$ etch solution (Copper etch, Transene) until the copper was gone by visual inspection, approximately 1.5h. This copper-free piece (Gr/PEVA) was transferred to a ≥18MΩ-cm resistivity water bath for 1h before transfer to a second clean water bath were it was left for 12h. After transfer to a final fresh water bath, the stack was pulled onto the appropriate sensor substrate and dried using a gentle stream of nitrogen.

The sensors used as controls were fabricated using similar transfer techniques. Solutions of 4 wt. % PEVA and 1 wt. % CB were sonicated for 2-4h until well dispersed. The solution was then spun onto bare copper and transferred as before or applied to the sensors using an airbrush. Graphene with no PEVA coating was transferred with a supporting layer of 495K A4 polymethyl methacrylate (PMMA, MicroChem) spun at 3000 rpm for 60 s. After transfer, the PMMA was removed by soaking the sensor in acetone for 10 minutes.

Instrumentation

Sensors were tested using a custom setup that has been described previously. Nitrogen was used as a carrier gas through the bubblers at a flow rate of 3000 mL/min. Organic vapors were generated by sparging N_2(g) through 45 cm tall bubblers that had been filled with the appropriate solvents. The analyte concentration was controlled by adjusting the volumetric mixing ratio of the saturated analyte stream to the background N_2(g) stream. The flow rates of the background and analyte gases were regulated using mass flow controllers. Each run started with a 700 s background collection. Each analyte exposure consisted of 200 s of pure background gas, 80 s of diluted analyte, and then 200 s of background gas to purge the system. The sensors were loaded into a rectangular, 16-slot chamber connected by Teflon tubing to the gas delivery system. The resistance of each of the sensors in the array was measured by a Keithley 2002 multimeter coupled to a Keithley 7001 multiplexer. The measurement electronics were interfaced with a computer via a GPIB connection and were controlled with LabVIEW software.

Profilometry data of the polymer overlayers was collected on a Bruker Dektak XT profilometer using a probe with a 2 μm tip radius. Atomic force microscope images of the sensors were collected using a Bruker Dimension Icon atomic force microscope. Raman spectra were collected with a Renishaw Raman microscope at λ=532 nm through an objective with numerical aperture=0.75. The laser power was ~3 mW.

Results

Figure 1 shows the response of a sensor coated with Gr/PEVA to a single pulse of vapor. Upon exposure of the sensor to the analyte, the resistance steadily increases until the analyte is purged from the chamber, at which point the resistance decreases back to the baseline value. The response from this sensor is quantified as the change in

resistance (ΔR) with respect to the resistance of the baseline (R_b), shown below in Equation 1, where R_p is the peak resistance of the sensor.

$$S = \frac{R_p - R_b}{R_b} * 100 = \frac{\Delta R}{R_b} * 100 \quad (1)$$

The responses for all sensors in this work will be reported as $\Delta R/R_b$.

Several sets of control sensors were fabricated to compare with the optimized sensor design. Typical polymer composite sensors contain carbon black (CB) as a conductive material. The percent composition by weight of CB determines the baseline resistance and the optimal sensor response. The sensors in this work replace CB with a conductive monolayer of graphene. The control samples included graphene alone on a flat substrate, graphene on 150 nm columns, PEVA/CB transferred in various ways to flat substrates and substrates with columns (Figure 2). The sensors fabricated in this work on a substrate with 150 nm columns show the best response by far (Figure 3). Strikingly, the PEVA/CB composite sprayed onto the surface of a substrate shows a strong negative response to ethanol and ethyl acetate, behavior which has been reported previously for these sensors.[5] However, the PEVA/CB composites formed as uniform films show a positive response instead.

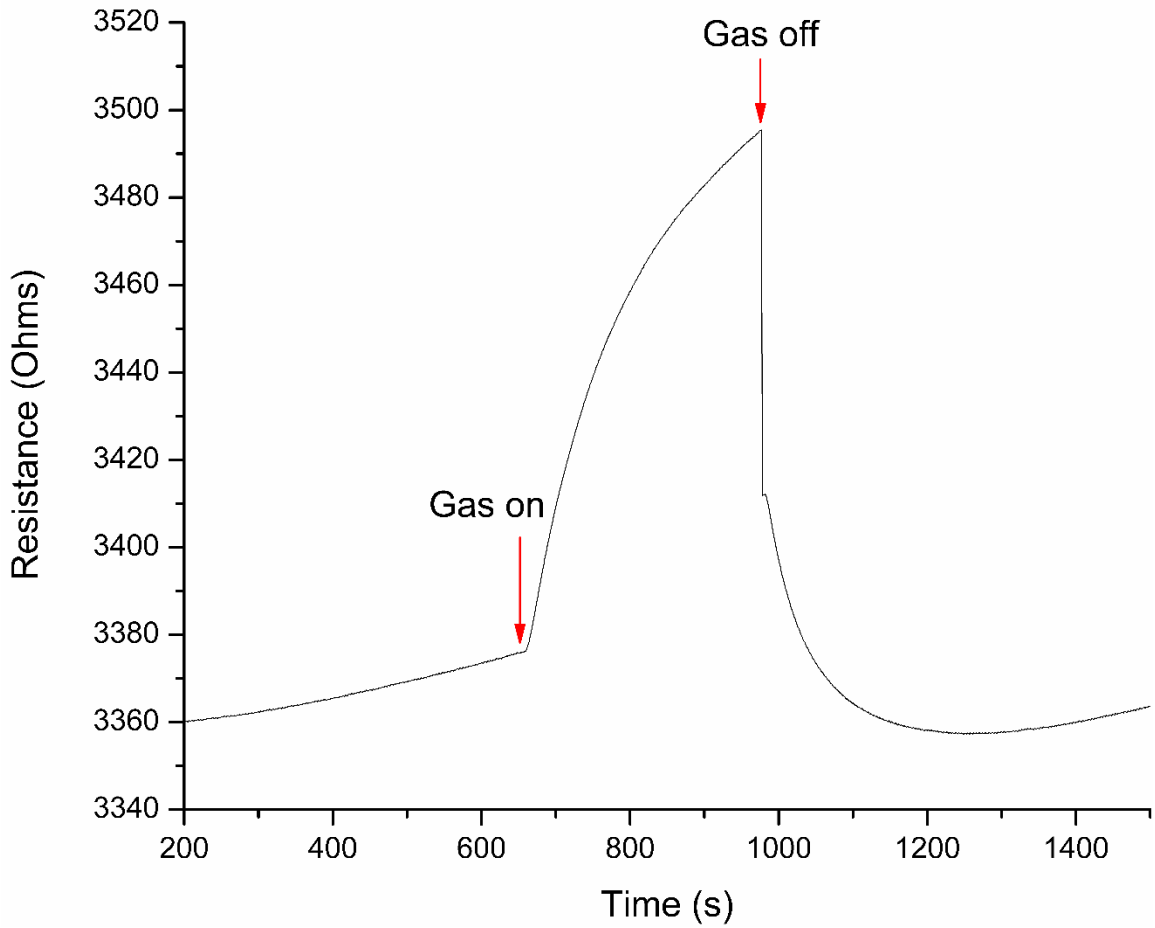

Figure 1. A typical sensor response. The points at which the sensor was exposed to the analyte and purged with the carrier gas are marked above.

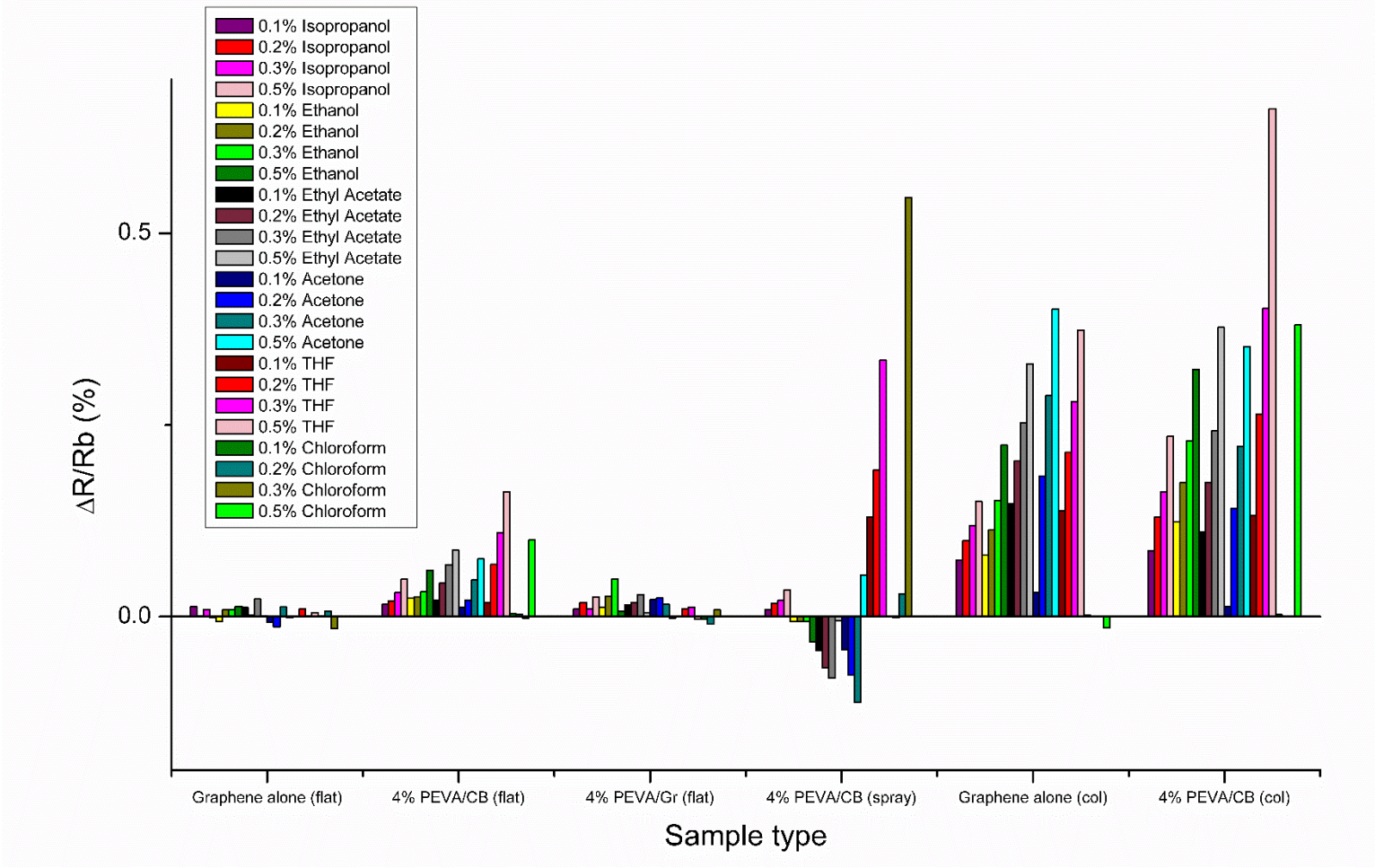

Figure 2. Responses from control sensors. The type of material the sensing material is shown below the x-axis with the type of substrate listed in parentheses. Textured substrates with columns are abbreviated as (col) while flat substrates are (flat).

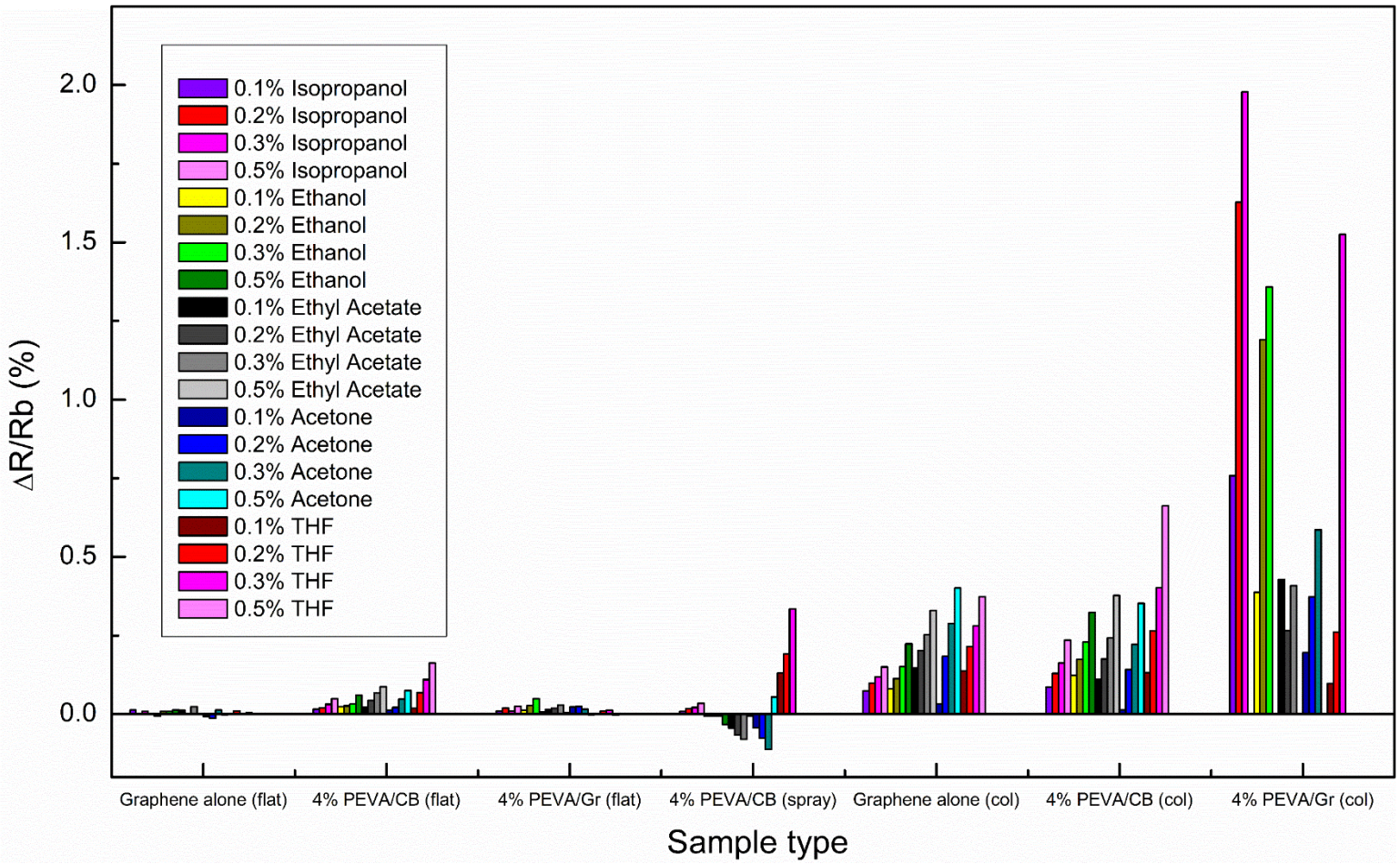

Figure 3. Control sensors versus PEVA/Gr on columns (far right). The best response comes from the PEVA-graphene film on a glass substrate with 150 nm high columns with a 3 μm diameter and 7 μm pitch. This design outperforms PEVA-CB and graphene alone.

The sensors in this work were optimized for the ideal thickness of the polymer overlayer (Figure 4). A spin curve for the 4 wt. % PEVA solution in toluene shows the expected dependence of thickness, which goes as the square root of the speed. Figure 4b shows the responses for sensors with the polymer overlayer spun on at speed between 1000 and 8000 rpm. Although the thickest layer (~320 nm) showed a strong response to various analyte, the responses increase significantly for sensors with thinner layers of PEVA.

The sensors were similarly optimized for the number of columns on the substrate, shown in Figure 5. The standard pattern were columns with 3 μm diameter and a pitch of 7 μm. The pitch was then varied between 7 and 120 μm with a constant thickness of polymer overlayer and size of the Gr/PEVA sheet transferred. As the number of columns decreased, so did sensor response. Figure 5b shows the response with respect to the number of columns and show a plateau around 500,000 columns.

The reproducibility of the responses of the optimized sensor was also probed through repeated measurements of response to the same amount of analyte. Figure 7 shows the response of an optimized sensor upon repeated exposures to 0.3% acetone. The response decreases over time to a plateau at 60% of the original signal, but after being allowed to rest, the sensor recovers the full response seen initially.

Raman spectra were collected for a sensor in contact with a 0.3% exposure of acetone. Figure 7 shows the response before and after exposure to the analyte. The G and 2D peaks of graphene can be seen. An additional broad peak from the substrate can be seen at 2400 cm^{-1}. This substrate peak does not shift upon exposure, while the 2D and G peaks shift significantly higher in energy upon exposure. The shift to higher energies is indicative of contraction of the lattice (Figure 7a).

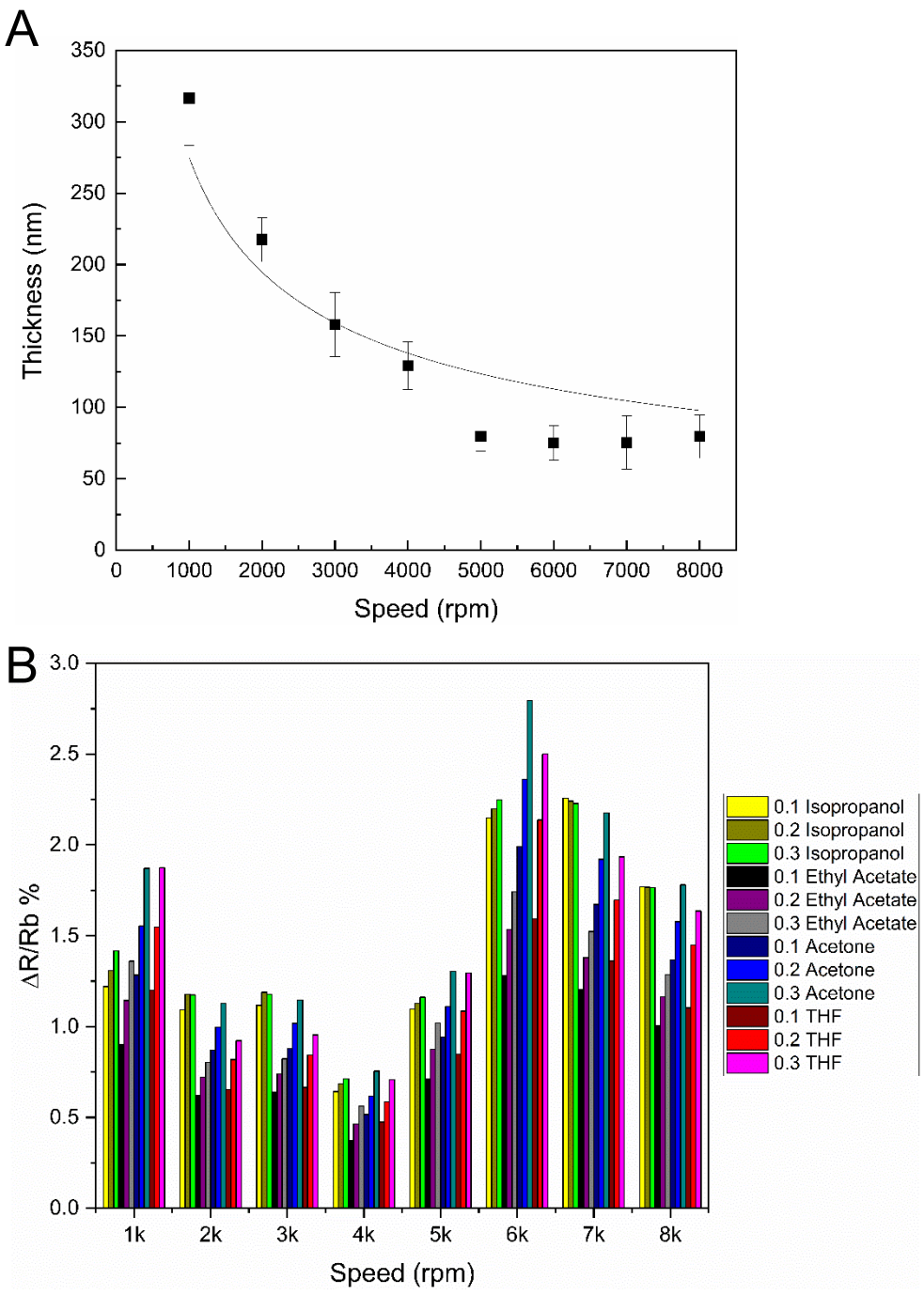

Figure 4. Effect of polymer overlayer on response. A) Polymer spin curve for a 4 wt. % solution of PEVA in toluene. B) Responses for different thicknesses of polymer. The best sensitivity and response is seen from the samples spun at 6000 rpm.

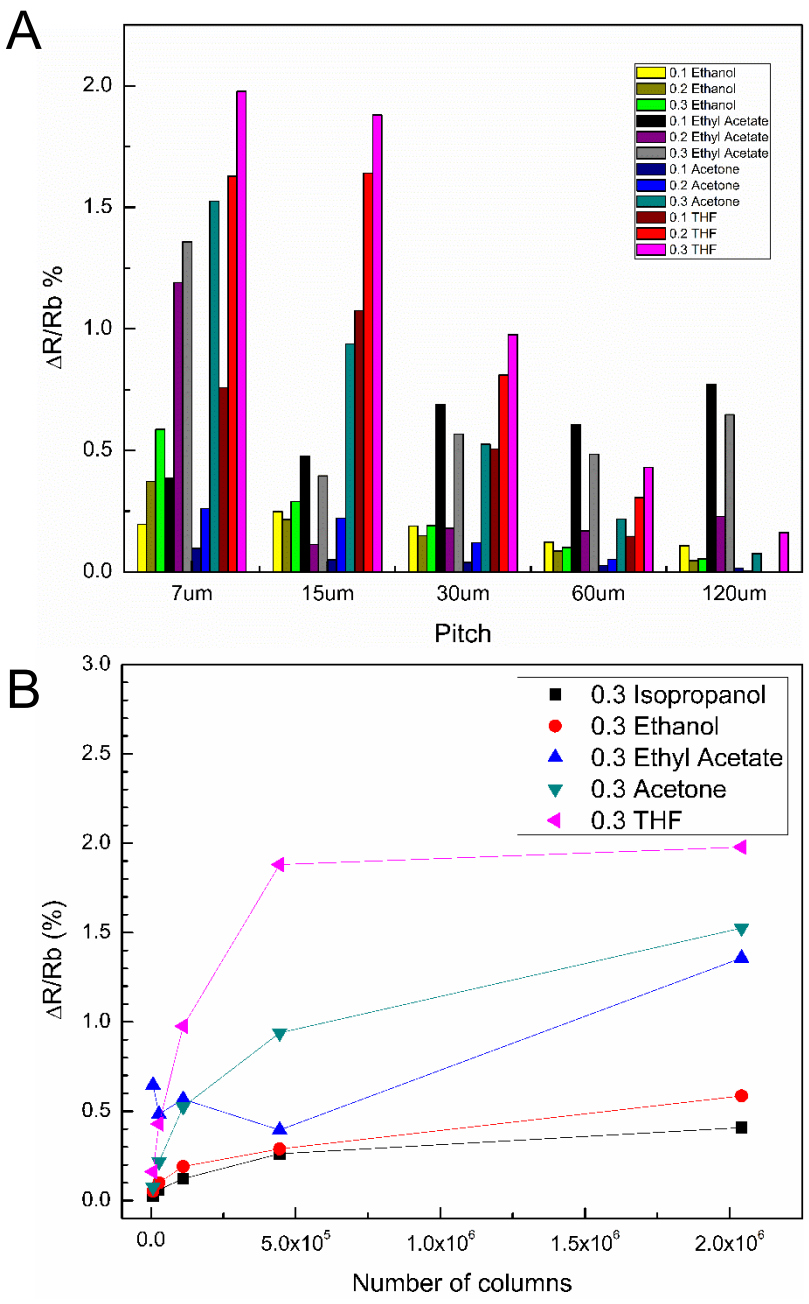

Figure 5. Effect of pitch on response. A) Comparison of responses with changing pitch. More closely spaced columns improve the response of the film. B) While the number of columns makes a large difference initially, the magnitude of response begins to plateau after enough columns are added.

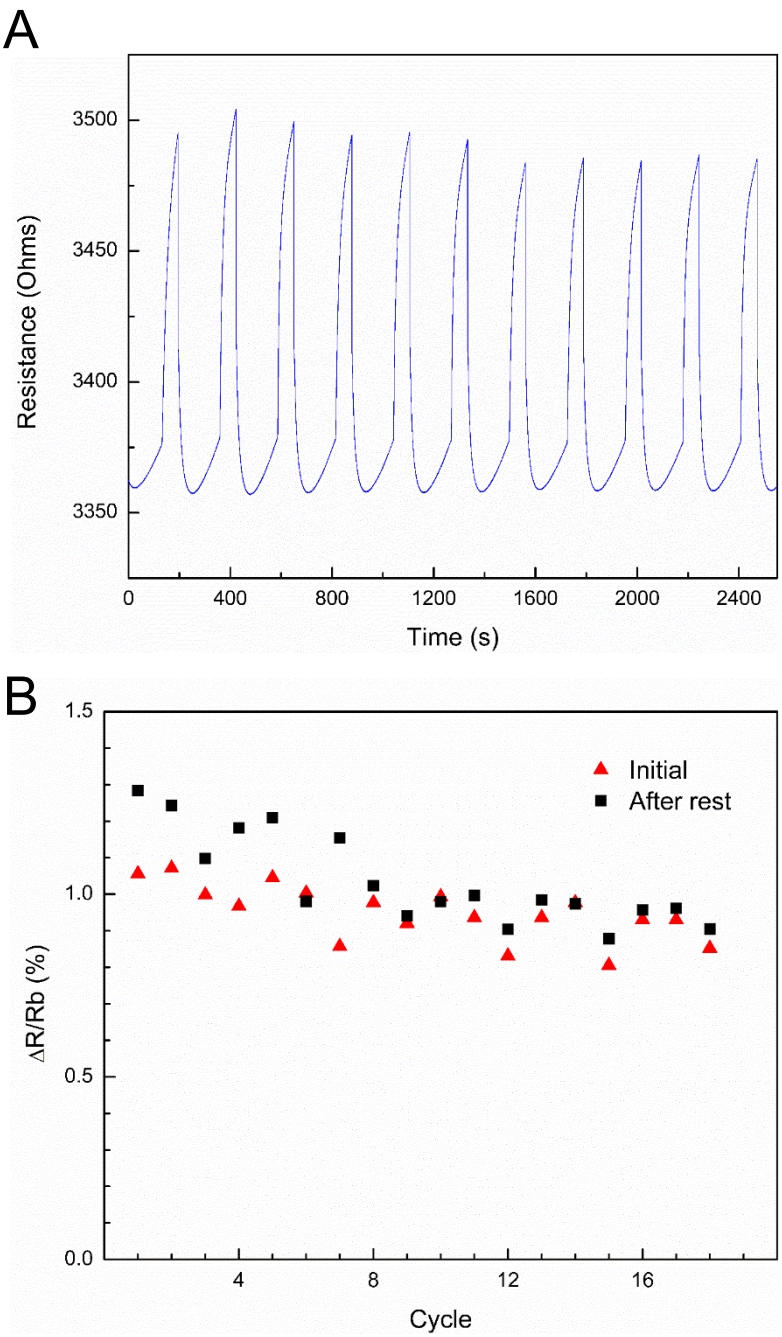

Figure 6. Stability of the polymer-graphene chemiresistors. A) Change in 0.3% acetone response versus time. Although the magnitude of the response decreases slightly, the shape of the response does not change over repeated exposures. B) Initial responses to 0.3% acetone compared to the same exposures after letting the sensor rest for an hour. The response fully recovers after this prolonged rest.

A

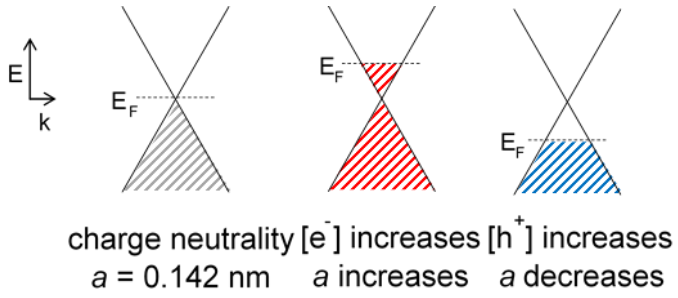

B

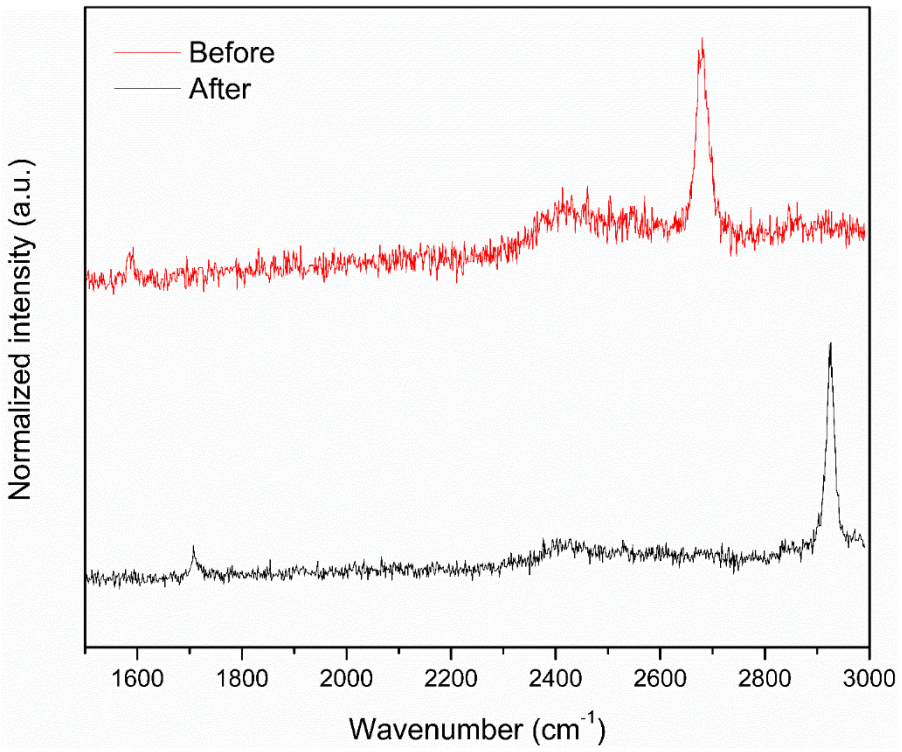

Figure 7. Raman at a representative spot on a sensor. A) How a lattice change in graphene is related to the shift in Fermi level. B) Before exposure to acetone, the G peak (1580 cm^{-1}) and 2D peak (2670 cm^{-1}) are visible. After exposure, both have shifted significantly to higher wavenumbers. This shift indicates that the graphene in this region has likely contracted, which leads to changing conductive pathways through the graphene, measured as a change in resistance.

Discussion

The response of the optimized sensors described here show a strong dependence on the number of columns (Figure 5). On this scale, increasing the number of columns leads to a higher response until a plateau is reached at 500,000 columns. This plateau indicates that on this scale that the resistance change in the graphene is limited by the degree of strain that an analyte can impose on the PEVA/Gr stack as more columns do not substantially enhance the signal. Response also depends on the thickness of the polymer overlayer, scaling proportional to the square root of the thickness (Figure 4). The optimal thickness is then around 70 nm, while the optimal spacing is columns with a 3 μm diameter and 7 μm pitch. While the signal does degrade overall, the sensors have highly reproducible signals but a long recovery time (Figure 6).

Raman spectroscopy has been established as the primary method to characterize strain in graphene. A Raman spectrum of pristine graphene has two main peaks, at 1560 cm^{-1} and 2700 cm^{-1}, which are labeled as the G and 2D peaks, respectively. Both arise from the breathing mode of the graphene lattice.[6] These characteristic peaks are very responsive to small perturbations in the electronic structure of the graphene lattice, such as any shift of the Fermi level of graphene (E_F). As strain is known to change the localization of electron density in graphene and shift E_F, compressive and tensile strain can readily be identified. Tensile strain leads to a red shift of the G peak on the order of hundreds of wavenumbers (cm^{-1}) while compressive strain leads to a slightly smaller blue shift of the G peak (around 20 cm^{-1}).[7] When the lattice is disrupted through the formation of defects, a third peak appears in the spectrum around 1320 cm^{-1} and is labeled the D peak. The intensity of the D peak correlates to the degree of lattice disruption.[8] Consequently, the introduction of defects to the lattice alters the Raman spectrum of graphene in an essentially orthogonal manner to strain-induced changes. The ratio of the intensity of the D peak to the G peak (I_D/I_G) can be used as a

metric for the growth of defects in the graphene while the shifts of the G and 2D peaks are indicative of a strained monolayer of graphene. However, it is important to note that any shift in E_F results in changes to the shifts of the G and 2D peak. Thus, it is particularly important to characterize the strained surface before and after functionalization to isolate any changes from the shift of E_F due to strain from those due to fabrication. Here the Raman spectrum (Figure 7) demonstrates that sensor exposed to analyte undergoes a significant shift in the Fermi level, indicative of a large change in the surface strain. When the analyte is removed, the original spectrum can be obtained. No permanent defects are introduced as only the 2D and G peaks are visible in both spectra.

Conclusion

This work demonstrates that polymer-coated monolayer graphene can be integrated with a simple textured electrode to produce a stronger response than a polymer-CB film or graphene alone. The response is controlled by the structure of the underlying substrate along with the thickness of the polymer overlayer. While this sensor has a long recovery time for successive tests, it recovers full functionality after rest period. Raman indicates that the monolayer of graphene is intact on the substrate and undergoes electronic changes when exposed to an analyte.

References

1. Lee, C., Wei, X., Kysar, J. W. & Hone, J. Measurement of the Elastic Properties and Intrinsic Strength of Monolayer Graphene. *Science* **321**, 385–388 (2008).
2. Deng, S. & Berry, V. Wrinkled, rippled and crumpled graphene: an overview of formation mechanism, electronic properties, and applications. *Mater. Today* **19**, 197–212 (2016).
3. Chen, W. *et al.* Controllable Fabrication of Large-Area Wrinkled Graphene on a Solution Surface. *ACS Appl. Mater. Interfaces* **8**, 10977–10984 (2016).
4. Jung, W.-B., Cho, K. M., Lee, W.-K., Odom, T. W. & Jung, H.-T. Universal Method for Creating Hierarchical Wrinkles on Thin-Film Surfaces. *ACS Appl. Mater. Interfaces* **10**, 1347–1355 (2018).
5. Doleman, B. J., Lonergan, M. C., Severin, E. J., Vaid, T. P. & Lewis, N. S. Quantitative study of the resolving power of arrays of carbon black-polymer composites in various vapor-sensing tasks. *Anal. Chem.* **70**, 4177–4190 (1998).
6. Ferrari, A. C. *et al.* Raman Spectrum of Graphene and Graphene Layers. *Phys. Rev. Lett.* **97**, 187401 (2006).
7. Bissett, M. A., Tsuji, M. & Ago, H. Strain engineering the properties of graphene and other two-dimensional crystals. *Phys. Chem. Chem. Phys.* **16**, 11124–11138 (2014).
8. Beams, R., Gustavo Cançado, L. & Novotny, L. Raman characterization of defects and dopants in graphene. *J. Phys. Condens. Matter* **27**, 083002 (2015).